IEEE Trans EMC
1991 pp. 105-112

Sensor and Simulation Notes
Note 319

An Incident Field Sensor for EMP Measurements

Everett G. Farr and Joseph S. Hofstra
The BDM Corporation

November 6, 1989

Abstract

This note describes the initial development of the Balanced Transmission-line Wave sensor. sensor is being developed to address the need for a directional sensor when dealing with olation issues at hybrid EMP simulators. A prototype sensor was designed and tested. It led good performance, with measured Front/Back ratios between 20 and 29 dB. This may be ate for many applications. There are, however, many variables left to explore, and it may be le to improve the Front/Back ratio with further work.

CLEARED FOR PUBLIC RELEASE
WL/PA 5/5/89
Amended by WL/PA as
89-186

319

IEEE Trans EMC
1991 pp. 105-112

WL-EMP-SSN-319

Sensor and Simulation Notes
Note 319

An Incident Field Sensor for EMP Measurements

Everett G. Farr and Joseph S. Hofstra
The BDM Corporation

November 6, 1989

Abstract

This note describes the initial development of the Balanced Transmission-line Wave sensor. This sensor is being developed to address the need for a directional sensor when dealing with extrapolation issues at hybrid EMP simulators. A prototype sensor was designed and tested. It provided good performance, with measured Front/Back ratios between 20 and 29 dB. This may be adequate for many applications. There are, however, many variables left to explore, and it may be possible to improve the Front/Back ratio with further work.

CLEARED FOR PUBLIC RELEASE
WL/PA 5/5/89

transmission lines, waveguides, electromagnetic pulse simulators

Amended by WL/PA 95
89-186

I. Introduction

When measuring fields at hybrid EMP simulators, it is often desirable to have a sensor that is directional. By this, we mean the sensor has a cardiod, or $1 + \cos\theta$ antenna pattern. This allows one to measure only to the incident field in an environment where both incident and reflected fields are present.

With currently available sensors, we are only able to measure total (incident + reflected) fields. There are times, however, when it would be useful to isolate the incident field from the total field. An example of this is when performing extrapolations at hybrid EMP simulators,[1] such as the ATHAMAS I simulator shown in Figure 1. This paper describes the development of a sensor that isolates the incident field from the total field.

The design of the sensor is based on an idea developed for a unidirectional EMP simulator[2]. By using this device as a receiving antenna instead of a transmitting antenna, a directional sensor is achieved. We call this sensor the Balanced Transmission-line Wave sensor, or BTW.

In this note a simplified theory of operation is discussed. Furthermore, experimental results are presented for two prototype sensors in a number of different types of tests. These results confirm the principle of operation of the sensor and encourage further engineering development of the BTW.

II. Approach

A simple view of a BTW is shown in Figure 2(a). It consists of a 100-Ω transmission line that tapers to a 100-Ω load on either end. This load can be either a 100-Ω resistor or a 100-Ω twinax cable. For structural reasons, an extra ground plane is normally inserted at the symmetry plane. In doing so, the 100-Ω resistors become two 50-Ω resistors, and the 100-Ω twinax terminations become two 50-Ω coax transmission lines.

The structure of Figure 2(a) has been analyzed in detail by Jiunn Yu, et. al. in Sensor and Simulation Note (SSN) 243. The treatment in SSN 243, however, is more complicated than what is required for a simple understanding of the BTW. We therefore begin with a simplified low-frequency explanation of how and why the device operates.

The BTW can be described most simply in terms of a parallel plate transmission line. This is later generalized to an arbitrary transmission-line configuration. We begin with the parallel plate model.

A. Parallel Plate Transmission Line Model

Consider the diagram of Figure 2(b). It consists simply of two closely spaced parallel plates that form a transmission line. Each end of the line is assumed to be terminated in the characteristic impedance of the line. We can describe the characteristics of the device in terms

[1] E. G. Farr, *Extrapolation of Ground-Alert Mode Data at Hybrid EMP Simulators*, Sensor and Simulation Note 311, July 1988.

[2] J. S. Yu, et.al., *Multipole Radiations: Formulation and Evaluation for Small EMP Simulators*, Sensor and Simulation Note 243, July 19 1978.

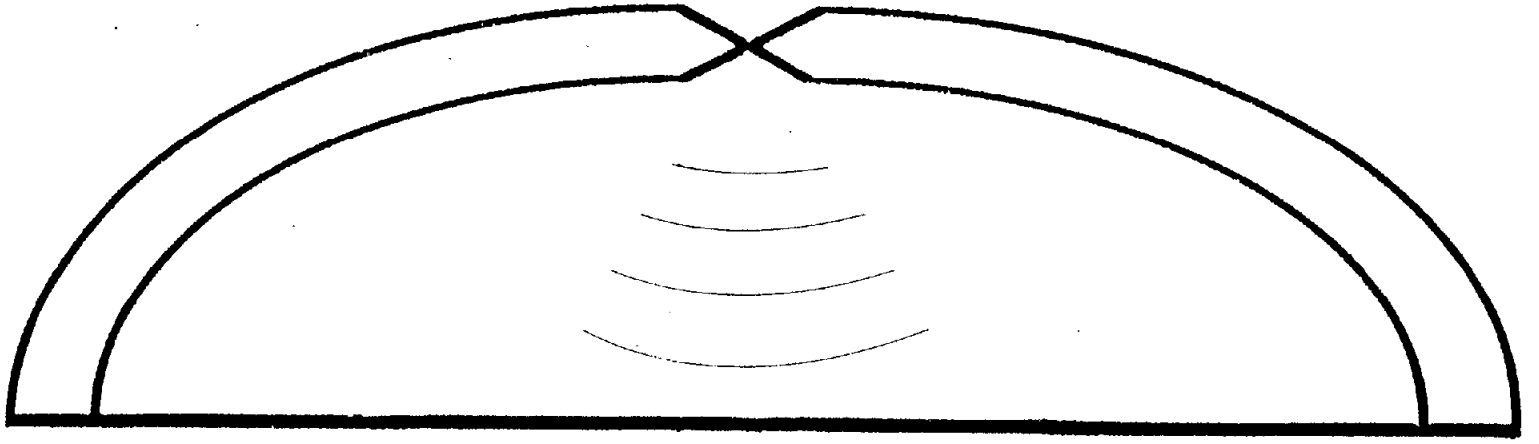

Figure 1. ATHAMAS I EMP Test Facility

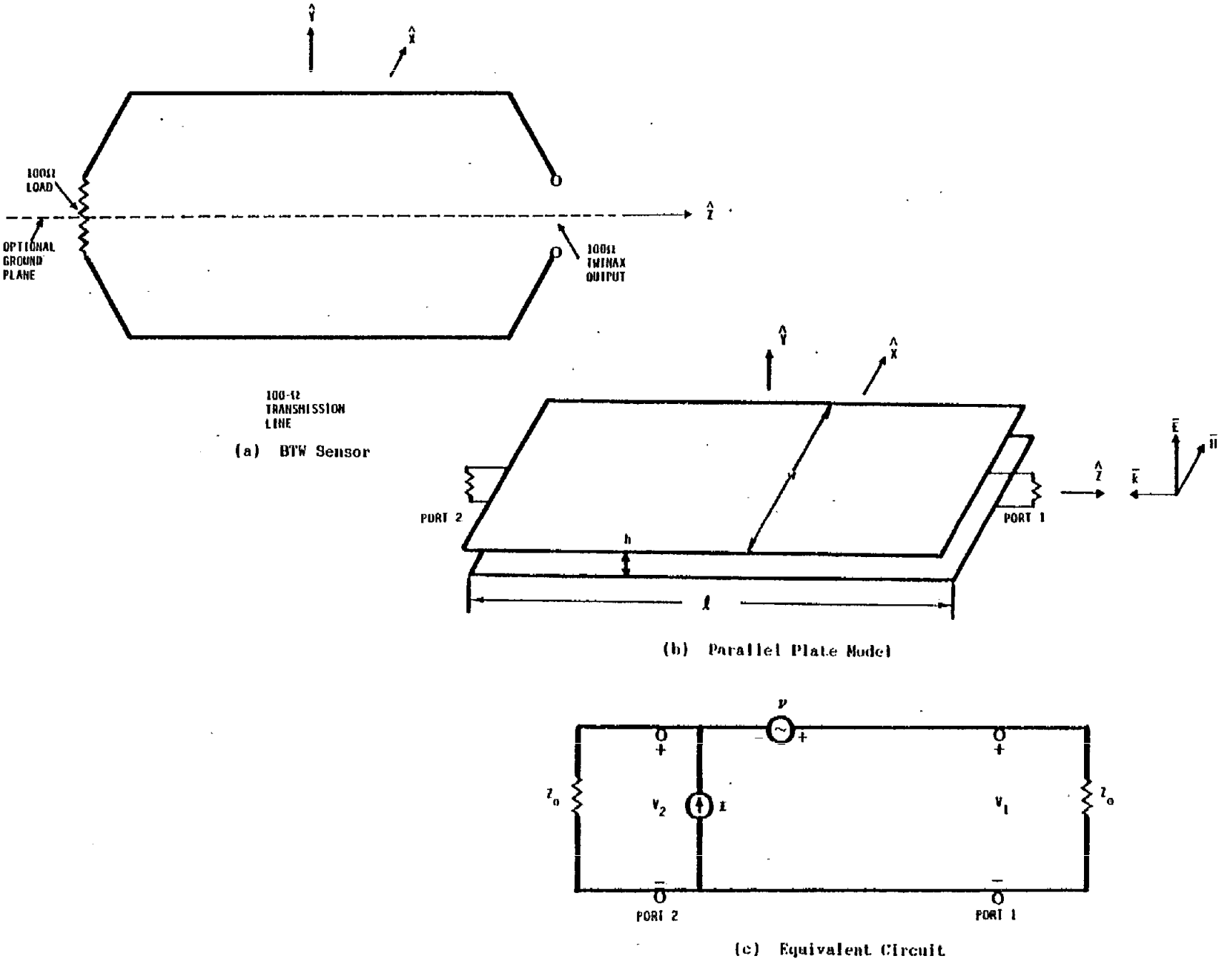

Figure 2. Simplified Diagram of the BTW Sensor(a), Parallel Plate Model (b) and Equivalent Circuit (c)

of a simple equivalent circuit, shown in Figure 2(c). This is a current and voltage source feeding into two matched loads. The voltage and current sources are derived from inductive and capacitive coupling, respectively.

First, we derive the voltage source due to inductive coupling. If a plane wave is incident upon the sensor as shown in Figure 2(b), then the induced voltage through the loop in the y-z plane is

$$\mathcal{V}(t) = -\bar{A} \cdot \frac{d\bar{B}}{dt} \tag{1}$$

where $\bar{A} = lh\hat{x}$. Since $\bar{B} = \mu_o H_x \hat{x}$, we can express the above as

$$\mathcal{V}(t) = -\mu_o \, lh \, \frac{dH_x}{dt} \tag{2}$$

where $\mu_o = 4\pi \times 10^{-7}$ H/m. This behavior is directly analogous to a B-dot sensor.

Next, we derive the current source due to capacitive coupling. For the configuration of Figure 2(b), the current induced between the plates is

$$\mathcal{I}(t) = C \, \frac{dV}{dt} \tag{3}$$

If we assume a uniform electric field between the plates, then the voltage between the plates is

$$V(t) = -h \, \hat{y} \cdot \bar{E}(t) \tag{4}$$

where $\bar{E}(t)$ is the electric field due to the incident field. If we also assume that fringing is negligible at the edge of the plates, then

$$C = \frac{\epsilon_o lw}{h} \tag{5}$$

where $\epsilon_o = 8.85 \times 10^{-12}$ F/m. Combining the above three equations, we find the current source as

$$\mathcal{I}(t) = -\epsilon_o \, lw \, \frac{dE_y}{dt} \tag{6}$$

It turns out that this current source can be simply expressed in terms of the voltage source, $\mathcal{V}(t)$. This is accomplished by assuming $E_y/H_x = \eta = \sqrt{\mu_o/\epsilon_o}$, where $\eta = 377\ \Omega$ is the impedance of free space. By doing this, we have

$$\mathcal{I}(t) = -\epsilon_o \eta \, lw \, \frac{dH_x}{dt} = -\frac{\mu_o \, lh \, \dfrac{dH_x}{dt}}{\eta \dfrac{h}{w}} \tag{7}$$

Since the characteristic impedance of a parallel plate transmission line is $Z_o = \eta h/w$ we have, by combining Equations (2) and (7)

$$\mathcal{I}(t) = \frac{\mathcal{V}(t)}{Z_o} \tag{8}$$

This is the desired result.

It is clear from Figure 2(c) that if Equation (8) is true, then the voltage at Port 1 of the sensor is

$$V_1(t) = \mathcal{V}(t) \tag{9}$$

whereas the voltage at Port 2 is

$$V_2(t) = 0 \tag{10}$$

This is the behavior required for a directional sensor. If the wave is incident from the $-\hat{z}$-direction, it is simple to show with symmetry that Port 2 is excited and Port 1 has no response.

B. Arbitrary Transmission Line Model

It is not necessary to have a parallel plate transmission line to observe the effect described in the previous section. We now demonstrate that the phenomenon remains valid with an arbitrary transmission line.

The critical result that needs to be proven is Equation (8). We need a more general expression for $\mathcal{I}(t)$. In general,

$$\mathcal{I}(t) = C_l l \frac{dV(t)}{dt} \tag{11}$$

where C_l is the capacitance per unit length of the transmission line, l is the length of the line, and $V(t)$ is as defined in Equation (4). Using Equation (4), we get

$$\mathcal{I}(t) = -h\, C_l\, l\, \hat{y} \cdot \frac{d\bar{E}(t)}{dt} = -hl\, C_l \frac{dE_y}{dt} = -hl\, C_l \eta \frac{dH_x}{dt} \tag{12}$$

Furthermore, $\mathcal{V}(t)$ is unchanged from Equation (2), since the area of the loop does not change. Thus, combining Equations (2) and (12), we find

$$\frac{\mathcal{V}(t)}{\mathcal{I}(t)} = \frac{\mu_o}{\eta C_l} = \frac{\sqrt{\mu_o \epsilon_o}}{C_l} = Z_o \tag{13}$$

The last equation follows from a definition of characteristic impedance that holds for all transmission lines with air dielectric. This confirms that Equation (8) is valid for a transmission line of arbitrary cross section, provided that its phase velocity is equal to the speed of light. This property allows some flexibility in the design of the sensor.

C. Sensor Bandwidth

The frequency bandwidth is of concern when attempting to use the BTW at higher frequencies. It is, however, a somewhat difficult number to define. For our purposes, a reasonable definition would be the frequency band over which a minimum Front/Back ratio is maintained. This turns out to be somewhat difficult to measure, since our measurements of Front/Back ratio are taken in pulse mode and not in CW mode.

With this in mind, our best definition of bandwidth is probably given by Carl Baum in Sensor and Simulation Note 8[3]. This was developed originally for an MGL sensor, and since there is an analogy between the performance of a BTW and MGL, this definition may be reasonable. According to SSN 8, the maximum frequency of operation is

$$f_{max} = \frac{1}{\pi \mathcal{T}_t} \tag{14}$$

[3]C. E. Baum, *Maximizing Frequency Response of a $\dot{B}$ Loop,* Sensor and Simulation Note 8, December 6, 1964.

where $\mathcal{T}_t$ is the round trip transit time of a signal on the sensor. If there is no dielectric in the transmission line, then $\mathcal{T}_t = 2l/c$, and

$$f_{max} = \frac{c}{2\pi l} \tag{15}$$

As an example, the BTW we designed could be built to have a length about 0.35 m if some extra lengths of transmission line were removed. For this length, the bandwidth would be about 135 MHz. Of course, the bandwidth could always be increased by decreasing the size of the BTW, which in turn would decrease the effective area of the BTW.

D. Design Considerations

A diagram of the BTW is shown in Figure 3. The effective area was designed to be close to that of an MGL-2, 0.01 m^2. This is the same as the area of the loop one sees when looking at the side view of the sensor. The ground plane acts as a structural support, and does not affect the fields due to symmetry.

The output of the BTW is two SMA connectors at Port 1, which are each connected by cable to one of the inputs of a differential mode fiber optic transmitter. In fact, it is possible to measure fields from both directions concurrently. This can be done by replacing the two 50-Ω loads at Port 2 with cables that are connected to a second fiber optic transmitter.

An incident field excites the end of the transmission line structure port closest to the direction of incidence. The cables from Port 1 are routed to the back end of the sensor in order to keep instrumentation behind the incident field.

III. Laboratory Measurements

Two experiments were performed in the laboratory to check the performance of the BTW. First, a Time Domain Reflectometry (TDR) measurement was performed in order to check the impedance matching between different sections of the sensor. We connected the TDR input to one side of Port 1, leaving the remaining connector of Port 1 and both connectors of Port 2 matched to 50-Ω loads.

Results for the TDR are shown in Figure 4. One can relate bumps in the TDR measurements to physical features of the structure. The maximum deviation from the zero line is about 50 mρ, or about 5 percent of the maximum possible reflection coefficient, which is 1.

Next, TEM cell measurements were performed. In derivative sensors, one expects to see the measured response increase proportionally with frequency, or 20 dB/decade. TEM cell measurements were made in order to confirm this.

A diagram of the experimental setup is shown in Figure 5. The BTW was placed in a TEM cell and the output was fed through a balun into a network analyzer. The output of the sensor was referenced to the total throughput of the TEM cell. The BTW was placed in a manner that would maximize the coupling into it.

Results are shown in Figure 6. The response increases at 20 dB/decade, exactly as it should.

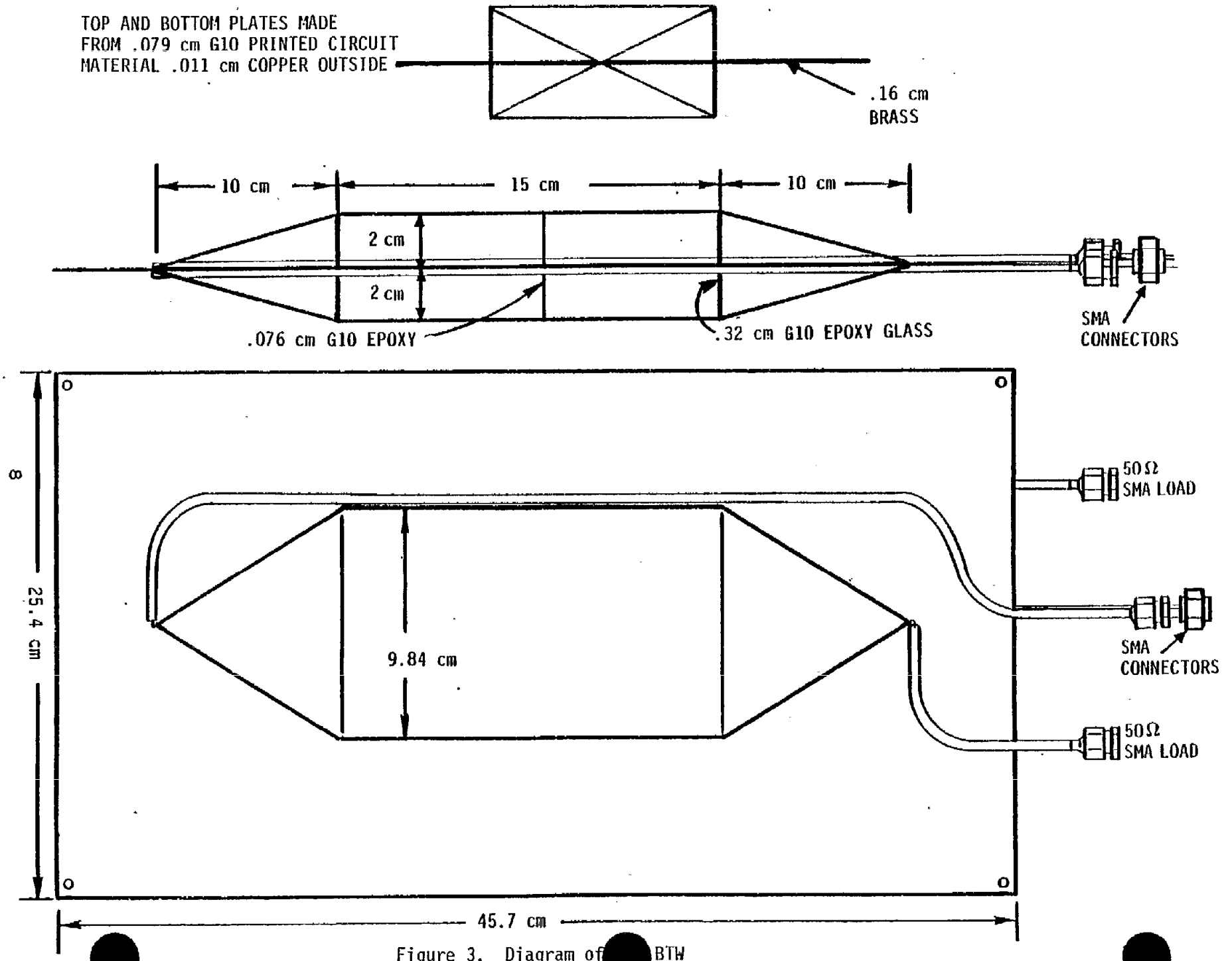

Figure 3. Diagram of BTW

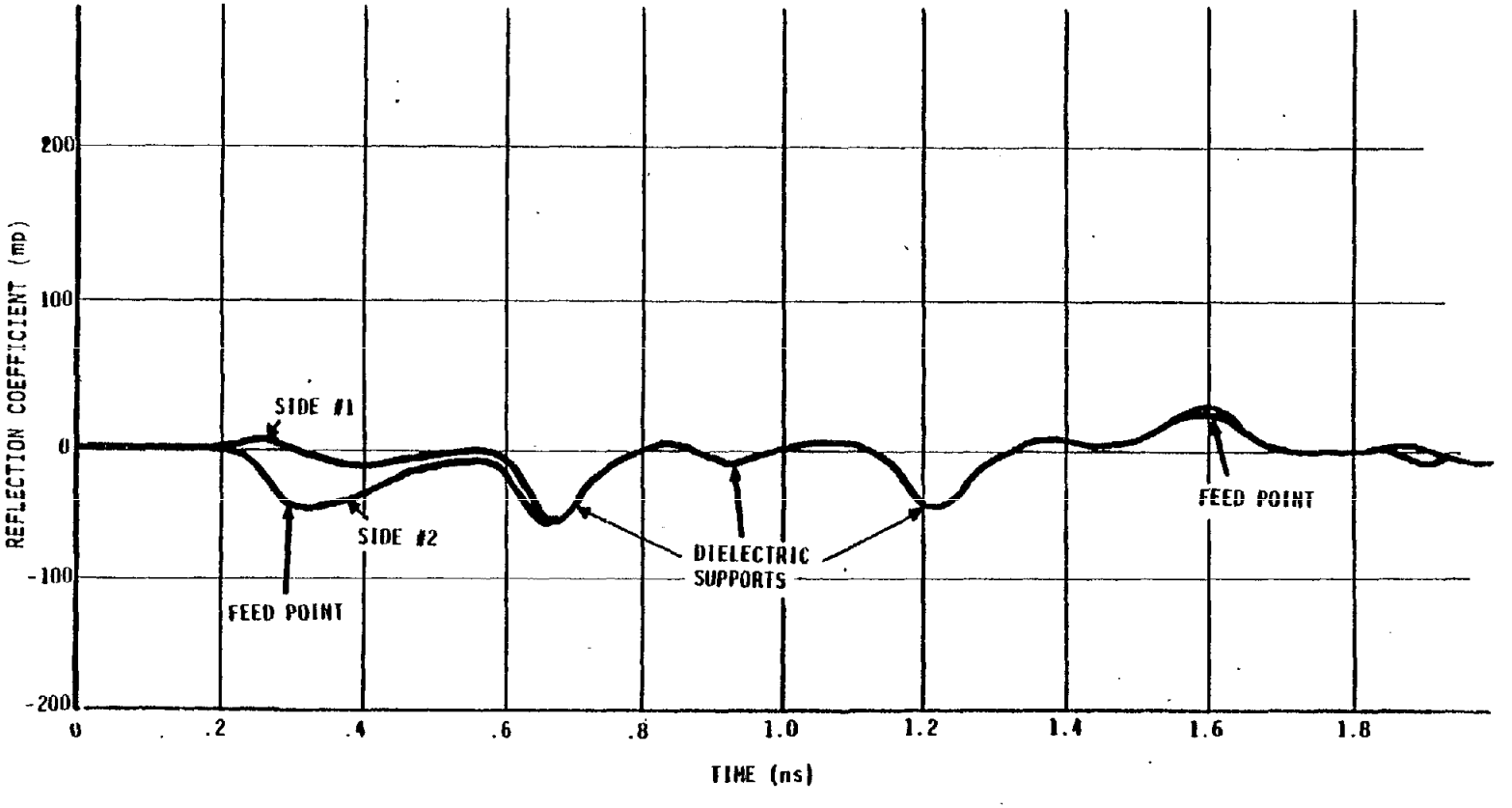

Figure 4. TDR of the BTW

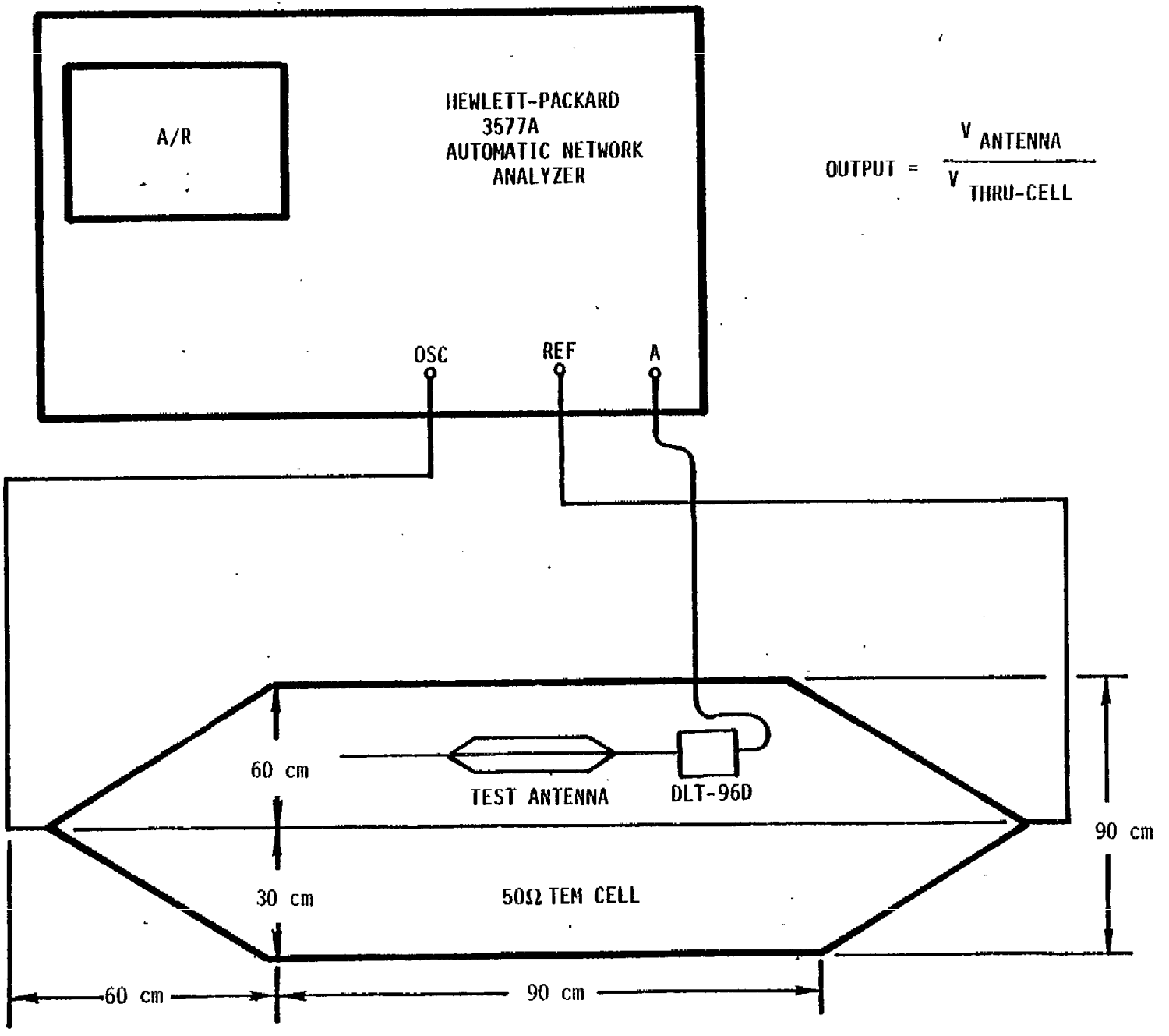

Figure 5. Instrumentation Setup for TEM Cell Measurements

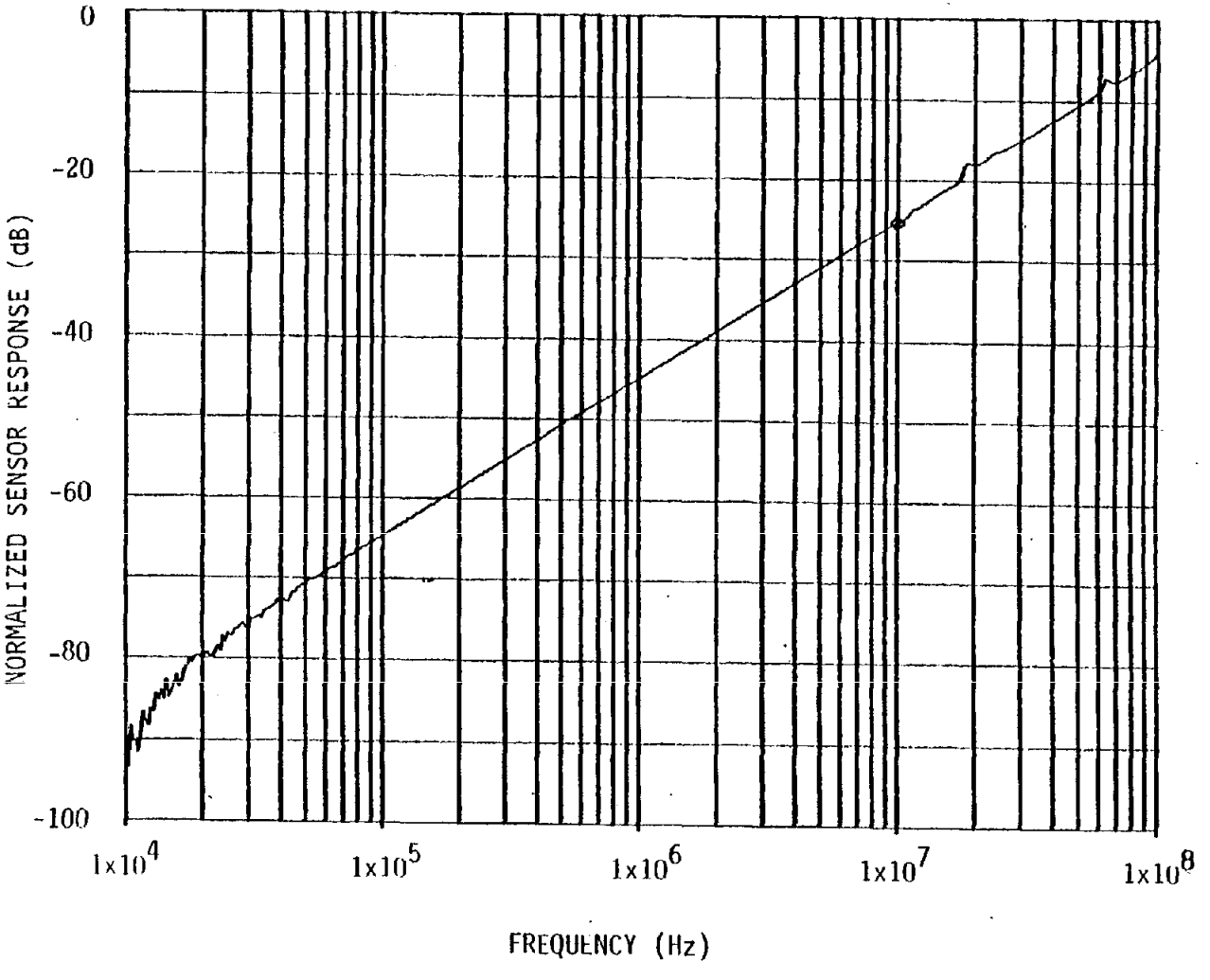

Figure 6. TEM Cell Sweep of the BTW

There are a few small bumps in the data in the decade between 10 and 100 MHz, but these are limitations of the TEM cell technique that normally occur at higher frequencies. This is simply demonstrated by replacing the cables with ones of a slightly different length and watching the bumps move to a different frequency.

IV. Experiments at ATHAMAS I

Two tests were performed at ATHAMAS I. First, measurements were made comparing a BTW to an MGL when used under the pulser in a normal mode of operation. Next, the BTW was pointed down in order to observe how well it rejected the incident field.

First, the response of the BTW was compared to that of an MGL-2 on the same shot, while both were positioned 5 m above the ground directly under the ATHAMAS I pulser. This is the normal mode of operation for the BTW. The BTW was directly under the pulser, while the MGL was 2 m outside the plane of the loop of the ATHAMAS I antenna. Since the ATHAMAS I pulser is 30 m high, this is effectively directly under the pulser.

For this experiment, the output of the BTW and MGL-2 were each fed directly into a differential mode Nanofast fiber optic links with 1 μs integrators turned on inside the transmitters. Since the output of the MGL is a twinax connector, a twinax-to-coax tee (TCT) was used to convert the twinax to two coaxial lines. The receivers fed into LeCroy 6880 A/D converters. Noise filters were turned on in the LeCroy digitizers at 150 MHz.

These data were processed using standard signal processing techniques. The zero line was found by averaging the first two hundred points. The effect of the fiber optic links was deconvolved from the output using standard Fourier transform techniques. Although we did not know exactly what the effective area of the BTW would be, we had to assume an effective area in order to get the data through the standard processing algorithms. For this reason, we assumed during our data processing that the effective area of the BTW was 0.01 m^2, as it was designed. Later, during testing at ALECS, we conducted an experiment to measure this quantity.

The waveforms measured with the MGL-2 and the BTW are shown in Figure 7. In comparing the two results, it is clear that the second large bump in the response of the MGL is the reflected field. It occurs at about 33 ns after the first peak, which is the two-way transit time between the sensor and the ground. The response of the BTW, however, is missing this second bump at 33 ns. There is a small difference in peak values of the two waveforms, and this indicates a small difference in the effective areas of the two sensors. Since the BTW was designed to have the same effective area as the MGL-2, this demonstrates the difference between the device as it was designed and as it was built.

Next, we placed the BTW pointing down, 5 m above the ground, in order to observe the rejection of the incident field. The sensors were placed on separate shots directly under the pulser, 5 m up. The same instrumentation and signal processing was used as before, except that a 150 MHz filter was introduced in data processing rather than in data acquisition.

A plot of the measured field is shown in Figure 8. Ideally, we expect to see the first 33 ns of the signal to be noise, with a large signal following that being the reflected field. Our measurment shows essentially this; the first 33 ns of the BTW signal is almost in the noise.

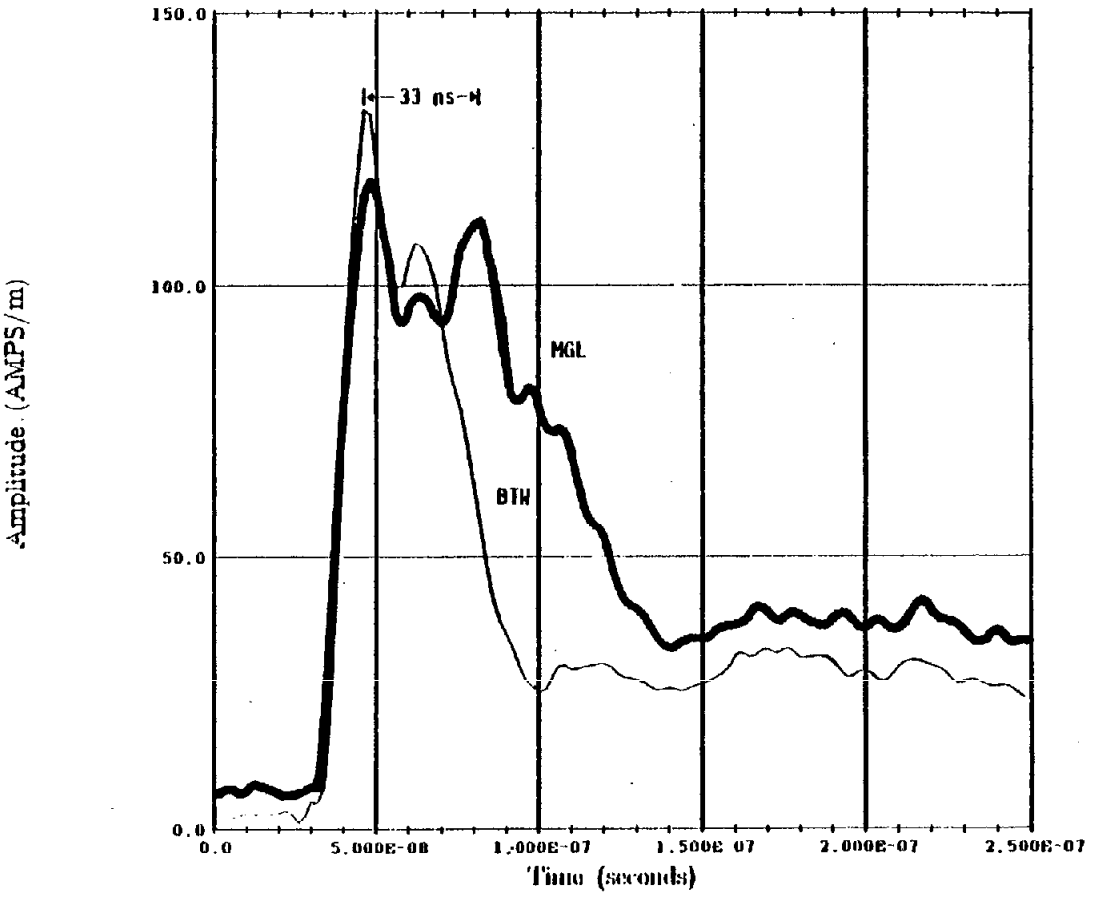

Figure 7. Fields Measured Under the ATHAMAS I Pulser With an MGL-2 and the BTW

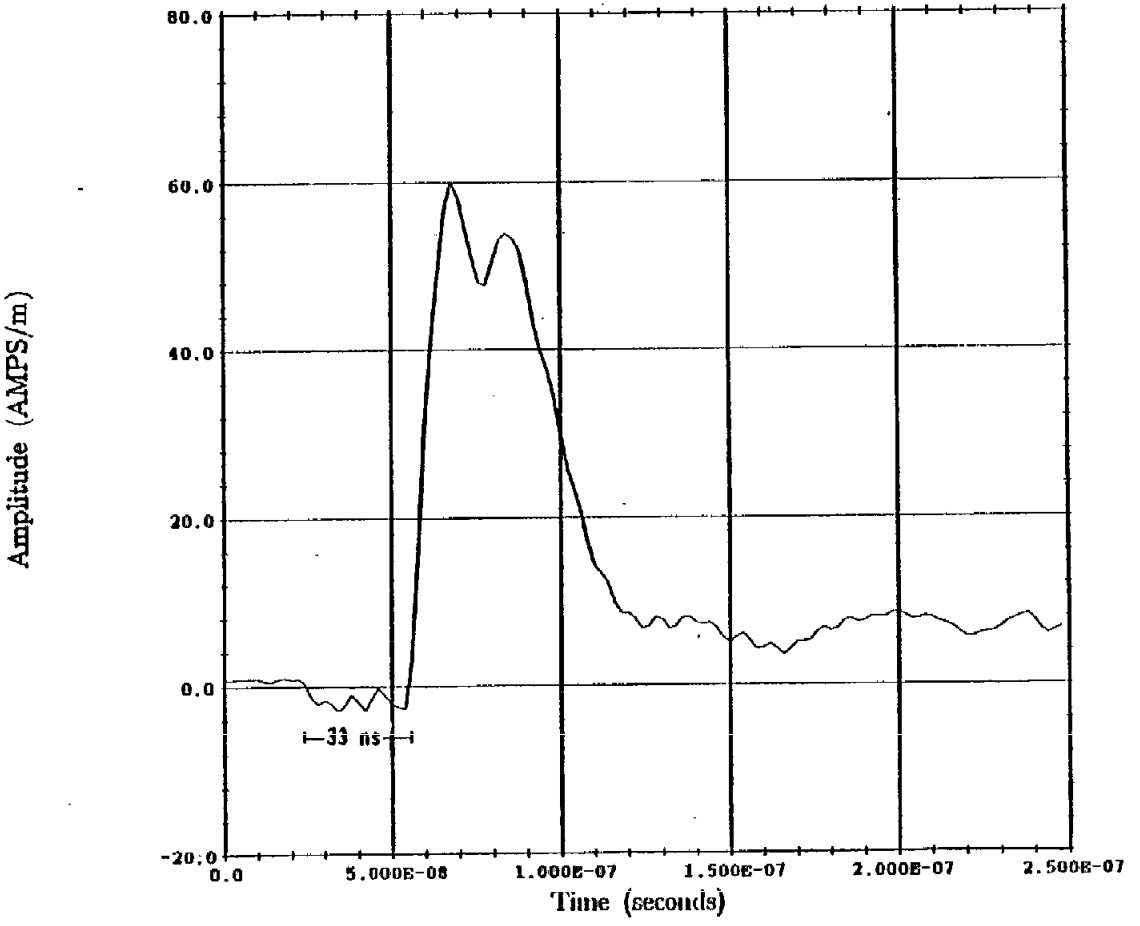

Figure 8. Rejection of the Incident Field at ATHAMAS I With the BTW

V. Experiments at ALECS

The final set of tests took place at ALECS. This facility was used because it is a transmission-line type simulator. As such, it provides a TEM field with almost no reflections. First, we attempted to calibrate the effective area of the BTW by comparing its response to that of an MGL. This was done with both integrated and derivative data. Next, we measured the Front/Back ratio of the BTW, again using both integrated and derivative data. Finally, we made measurements of the antenna pattern of the BTW in the E- and H-planes.

A. Effective Area Calibration

The first test was to compare the effective area of the BTW tapered design to that of an MGL-2. If we believe the effective area of the MGL-2 is 0.01m^2, then we should be able to use the ratio of the two peak magnitudes on the same shot to determine the effective area of the BTW.

An MGL-2 and the BTW were placed 2 m apart in the center of the testing volume. These sensors were each fed into a differential mode fiber optic link with the 1 μs integrators turned on. The connection to the link for the MGL required a TCT to split the twinax output into into two coaxial lines. The output of the fiber optic receivers was then fed into an active signal divider, which splits the signal into three parts and sends it on to three Tektronix 7912 digitizers.

Signal processing involved the normal process of finding the zero line by averaging the first fifty points and then deconvolving the effect of the fiber optic transmitter. As before, we assumed an effective area of 0.01 m^2 for the BTW to get the data through processing. We can calculate the correction needed in the effective area if we start with an assumed value for it.

The peak magnitude as measured with the BTW was compared to that measured with the MGL-2 for four shots. The average normalized peak magnitude of the field measured with the BTW was 1.1. This means that the effective area of the BTW is 10 percent larger than that of the MGL-2, or 0.011 m^2. A summary of this data appears in Table 1.

This process was then repeated with the integrators turned off. The signal processing involved only time tying, finding the baseline, and then linear scaling by a factor of $1/(\mu_o A_e)$. Again, a normalized peak was calculated by comparing the peak of the BTW data to that of the MGL-2 data. The average normalized peak magnitude of the field measured with the BTW was 1.15. This means that the effective area of the BTW is 15 percent larger than that of the MGL-2, or 0.0115 m^2.

There is some question as to which technique is more accurate, since we get a 5 percent difference in effective areas with the two techniques. This is especially true since the data in general do not have a wide scatter about their means. Normally, one would prefer to use the data that has the fewest signal conditioners to be deconvolved out. This suggests that the derivative data is more accurate, since it does not use an integrator. This does not explain, however, why there should be a discrepancy between the integrated and derivative data. Perhaps a reasonable compromise would be to take the average of the two techniques, which is 0.012. This is the effective area we used in the Front/Back ratio measurements.

Table 1. Effective area and Front/Back ratio at ALECS

Data Type	Effective Area (m^2)	Front/Back (dB)
Integrated	0.0110	20
Derivative	0.0115	29

B. Front/Back Ratio Measurements

The next experiment involved a measurement of the Front/Back ratio. This was done with both derivative and integrated measurements, using identical test setups and signal processing as in the previous experiment. The only difference is that the BTW was pointed away from the pulser instead of toward it. By using the peak magnitudes and correcting for the difference in effective areas between the MGL and BTW, one can calculate a Front/Back ratio.

The peak magnitude of a waveform with the BTW pointing backward was compared to the peak magnitude for an MGL over several shots. After taking into account the different effective areas between the MGL and BTW, there is an average of 20 dB Front/Back ratio with integrated data.

The same experiment was then repeated with derivative data. This time we found a Front/Back ratio of 29 dB. As in the previous experiment, we obtained different results for the integrated and derivative data. This time, however, the difference in results was more significant, 9 dB. One way to resolve the issue might be to assume that the simplest experiment, i.e., the one with derivative data, is the most accurate. It is a little difficult to say this definitively, however, and it will have to be left for future investigation.

C. Antenna Pattern Cuts

In the final experiment, we measured the antenna pattern of the BTW. For far field measurements, the BTW should have an antenna pattern that is $1 + \cos\theta$, according to SSN 243. This behavior should hold both in the E- and H-planes.

The data taken was all integrated, with all the instrumentation and signal processing the same as that for all previous integrated data taken at ALECS. Plots of the cuts are given in Figures 9 and 10. It is clear that the sensor performs about as we expect, with the exception near 180 degrees. We should remember, however, that the Front/Back ratio with derivative data was 9 dB better than that for integrated data, so if we had made these plots with derivative data we would expect better agreement at 180 degrees. Finally, we note that each of the points on these graphs was generated with a single shot, not an average over several shots. Therefore, we might expect a few points would be slightly different from theory.

VI. Error Analysis

Having demonstrated a Front/Back ratio of 20-29 dB, we now wish to demonstrate that this is reasonable. We should preface this section with the caveat that our technique for measuring the Front/Back ratio is approximate, since we measured it in the time domain using peak fields. Ordinarily one would want to measure this quantity in the frequency domain, since it can be expected to vary with frequency.

The first source of error in the design of the BTW is the dielectric supports made of G-10 printed circuit board. These supports increase the sensitivity of the BTW to electric fields by increasing the capacitance, while leaving unchanged the BTW's sensitivity to magnetic fields. The

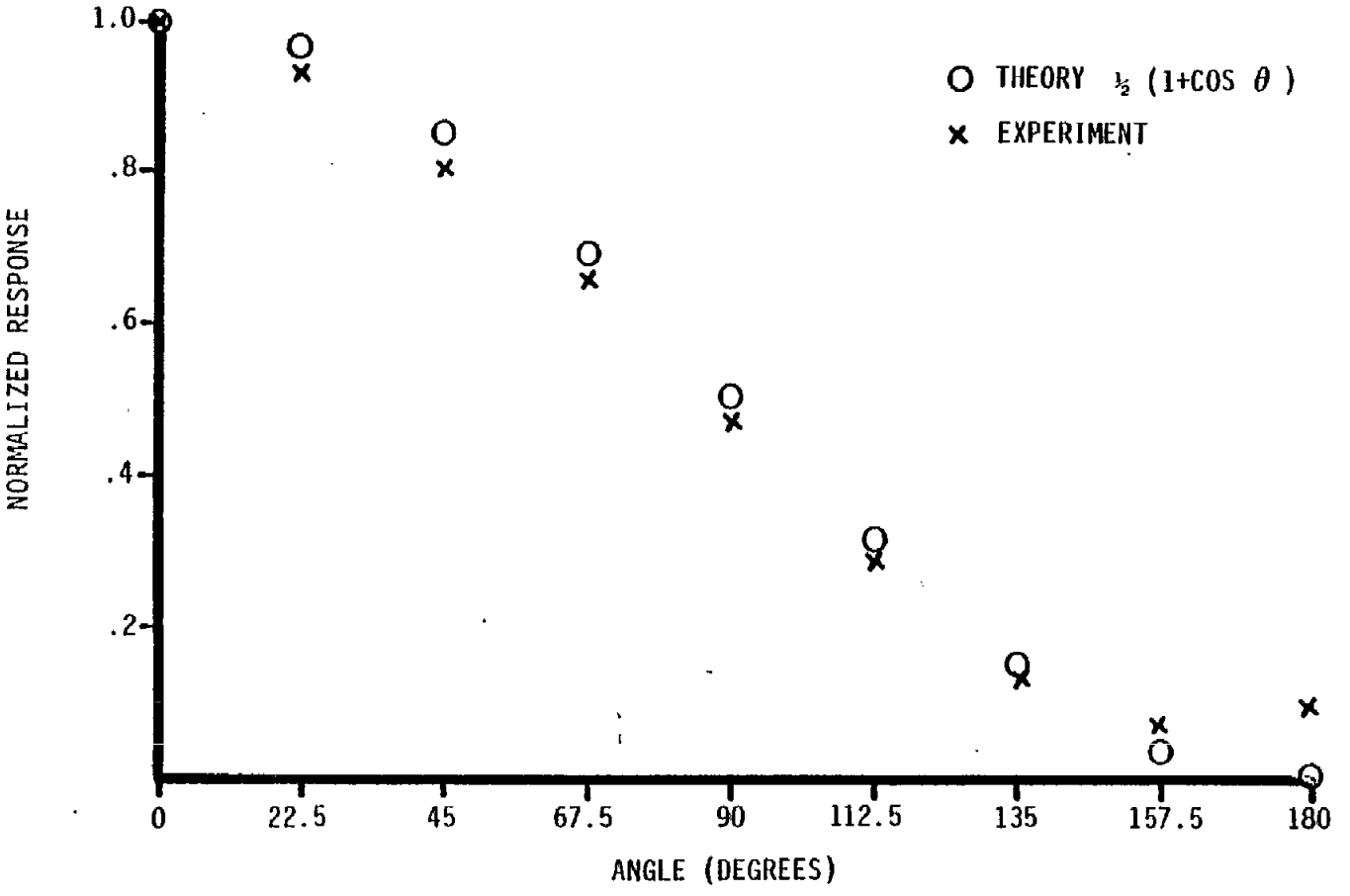

Figure 9. H-Plane Cut of the BTW Measured at ALECS

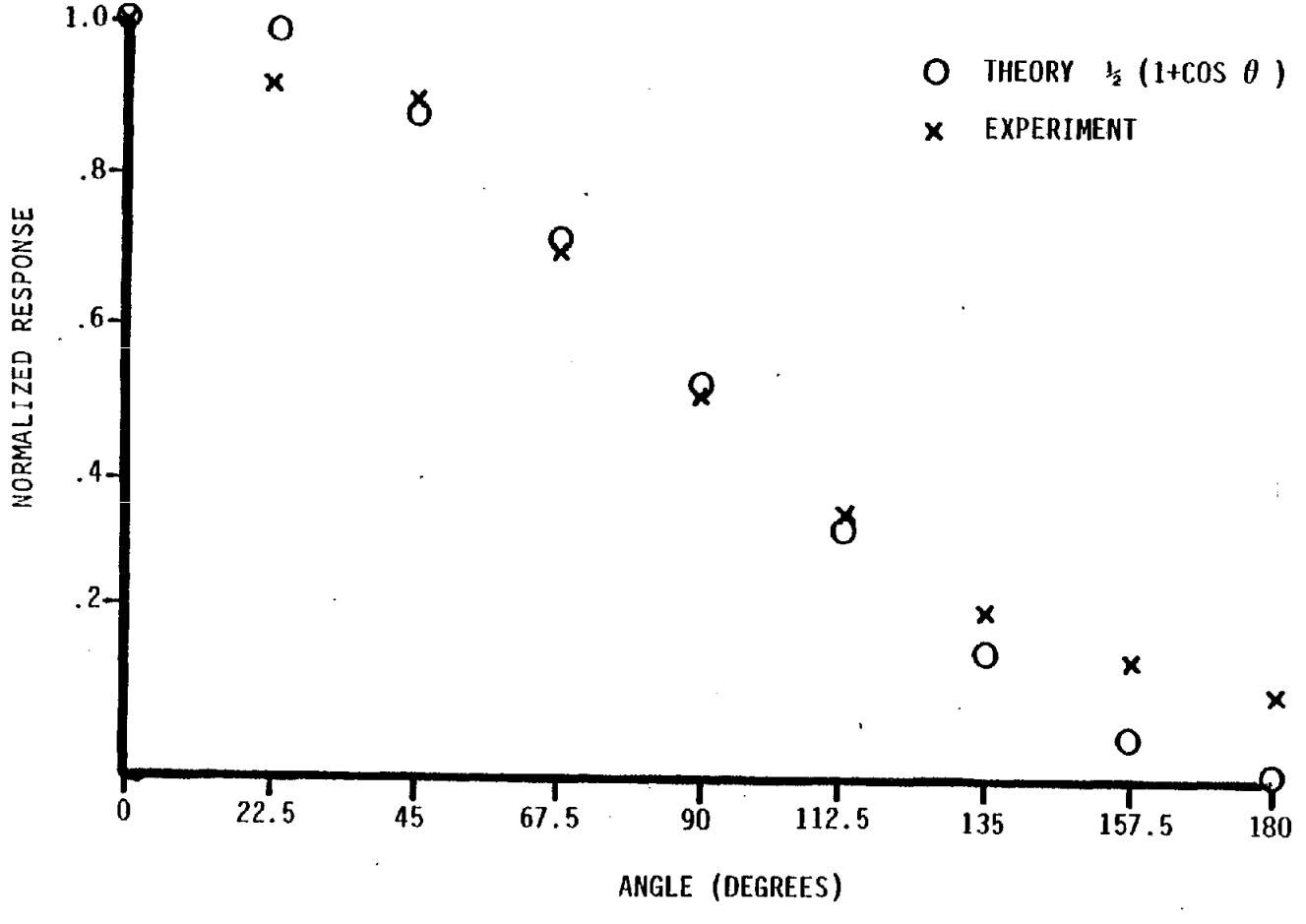

Figure 10. E-Plane Cut of the BTW Measured at ALECS

37 (20)

relative increase in capacitance is

$$\frac{\Delta C}{C} = (\epsilon_r - 1)\frac{A_d}{A} \tag{16}$$

where A_d is the area of the dielectric supports subtended by the $\hat{x}$-$\hat{z}$ plane, and A is the total area. For our sensor, $A \approx 250\text{cm}^2$, $A_d \approx 7.1\text{cm}^2$, and $\epsilon_r \approx 5$. Using these values,

$$\frac{\Delta C}{C} \approx 0.11 \tag{17}$$

Thus, the sensitivity of the BTW to electric fields is enhanced by about 11 percent. This leads to a Front/Back ratio of

$$F/B = \frac{E+\eta H}{E-\eta H} = \frac{E/\eta H + 1}{E/\eta H - 1} \approx \frac{1.11+1}{1.11-1} \approx 19 \approx 26 \text{ dB} \tag{18}$$

Thus, our observed Front/Back ratio is consistent with what we expect.

There are several additional factors that could contribute to errors in the BTW. One of these is the abrupt bend in the top and bottom plates at the end of the transitions. Another is the finite thickness of the ground plane. Another still is the perturbation of the fields due to the coaxial line lying on the ground plane. Clearly a more thorough study of these factors will be necessary if one needs a more accurate sensor.

VII. Conclusions

A prototype sensor has been developed that should simplify and improve the measurent of the incident field at hybrid EMP simulators. This sensor, the Balanced Transmission-line Wave sensor, has the property that it can measure the incident field while at the same time rejecting a reflected field. Preliminary measurements of the Front/Back ratio suggest an isolation of 29 dB with derivative data and 20 dB with integrated data.

There remain two areas where further investigation would be useful. The first is whether or not the Front/Back ratio can be improved with further experimentation. There are a number of design parameters that could be varied while maintaining the same overall response of the sensor. A systematic study of these variables may reveal designs with a larger Front/Back ratio. The second area where further investigation would be useful concerns the discrepancy between integrated and derivative measurements of Front/Back ratio. At some point, it will be necessary to generate a commonly accepted method of measuring this parameter.

An interesting aspect of this work is that is may have applications outside the area of EMP. It would seem there could be a number of uses for a broadband antenna that is both electrically small and directional.

Acknowledgement

We wish to express our appreciation to Carl Baum for his many helpful discussions on this topic. In addition, we wish to thank the Weapons Laboratory for funding this work.